

Comment on “Superconductivity in electron-doped layered TiNCl with variable interlayer coupling”

Dale R. Harshman

*Physikon Research Corporation, Lynden, Washington 98264, USA
and Department of Physics, University of Notre Dame, Notre Dame, Indiana 46556, USA*

Anthony T. Fiory

*Department of Physics, New Jersey Institute of Technology, Newark, New Jersey 07102, USA
(Received 3 June 2014; published 6 November 2014)*

In their article, Zhang *et al.* [*Phys. Rev. B* **86**, 024516 (2012)] present a remarkable result for $A_x(S)_y\text{TiNCl}$ compounds (α -phase TiNCl partially intercalated with alkali A and optionally co-intercalated molecular species S), finding the superconducting transition temperature T_c scales with d^{-1} , where the spacing d between TiNCl-layered structures depends on intercalant thickness. Recognizing that this behavior indicates interlayer coupling, Zhang *et al.* cite, among other papers, the interlayer Coulombic pairing mechanism picture [Harshman *et al.*, *J. Phys.: Condens. Matter* **23**, 295701 (2011)]. This Comment shows that superconductivity occurs by interactions between the chlorine layers of the TiNCl structure and the layers containing A_x , wherein the transverse A_x -Cl separation distance ζ is smaller than d . In the absence of pair-breaking interactions, the optimal transition temperature is modeled by $T_{c0} \propto (\sigma/A)^{1/2}\zeta^{-1}$, where σ/A is the fractional charge per area per formula unit. Particularly noteworthy are the rather marginally metallic trends in resistivities of $A_x(S)_y\text{TiNCl}$, indicating high scattering rates, which are expected to partially originate from remote Coulomb scattering (RCS) from the A_x ions. By modeling a small fraction of the RCS as inducing pair breaking, taken to cut off exponentially with ζ , observations of $T_c < T_{c0}$ are quantitatively described for compounds with $\zeta < 4 \text{ \AA}$ and $T_c \approx T_{c0}$ for $\text{Na}_{0.16}(S)_y\text{TiNCl}$ with propylene carbonate and butylene carbonate co-intercalants for which $\zeta > 7 \text{ \AA}$. Since a spatially separated alkali-ion layer is not formed in $\text{Li}_{0.13}\text{TiNCl}$, the observed T_c of 5.9 K is attributed to an intergrowth phase related to TiN ($T_c = 5.6 \text{ K}$).

DOI: [10.1103/PhysRevB.90.186501](https://doi.org/10.1103/PhysRevB.90.186501)

PACS number(s): 74.62.Dh, 74.10.+v, 74.25.fc, 74.62.Bf

I. INTRODUCTION

The layered compound TiNCl belongs to the group 4 metal-nitride halides of composition MNX with $M = \text{Ti, Zr, or Hf}$ and $X = \text{Cl, Br, or I}$, forming $X-(MN)_2-X$ layered structures with van der Waals bonding between twin halide layers ($X-X$). Pristine MNX compounds of principal crystal structures termed α and β forms are considered to be band insulators or wide-gap semiconductors [1–4]. Intercalation doping of a cationic element (A_x) between the halide layers, including co-intercalated molecular solvent species (S) $_y$, induces superconductivity in $A_x(S)_yMNX$ systems. Probably the most intriguing behavior observed is the strong correlation of T_c with the basal-plane separation d , defined as the periodicity distance along the c axis between $[MNX]_2$ blocks [5]. The subject paper by Zhang *et al.* [6] on $A_x(S)_y\text{TiNCl}$ compares eight compounds with relatively dilute doping x of an alkali element ($A = \text{Li, Na, K, and Rb}$) including four with co-intercalated molecules ($S = \text{THF, PC, and BC}$, denoting tetrahydrofuran, polypropylene carbonate, and butylene carbonate, respectively). The authors of Ref. [6] show that, with the exception of $\text{Li}_{0.13}\text{TiNCl}$, there exists a linear dependence between T_c and $1/d$, which is accepted as strong evidence of interlayer coupling, and suggest the relevance of our study of transition temperatures in high- T_c superconductors [7]. Data for T_c and d , as tabulated and read from Fig. 3 of Ref. [6], are listed in Table I.

II. T_c MODEL

For $A_x(S)_y\text{TiNCl}$, the interlayer interaction model follows from the identification of two types of layered charge reservoir

structures [7] in which the $[\text{TiNCl}]_2$ structure is proposed for type I and the intercalant layer $A_x(S)_y$ structure is proposed for type II, the latter including A_x intercalation at $y = 0$. The type-I reservoir hosts and sustains the superconducting current, whereas the type-II reservoir provides the mediation for the superconductive pairing interaction. In this model, the coupling occurs between adjacent ionic layers and thus involves the outer chlorine layers in $[\text{TiNCl}]_2$ and the alkali A_x in the intercalant layers. The optimal transition temperature T_{c0} occurs on the formation of participating charges in the two reservoirs for x at optimal doping.

These compounds present a unique situation among high- T_c materials in which the mediating layer adjacent to the superconducting condensate is incomplete, containing a high density of vacancies. Even without disorder in the $[\text{TiNCl}]_2$ bilayer structures [8], the close proximity of disordered A cations can induce remote Coulomb scattering (RCS) analogous to the depression of carrier mobility in two-dimensional systems by remote fixed charges [9]. Evidence for the presence of significant scattering are large resistivities at T_c and broad resistive transitions ΔT_c [6]. It is found herein that pair breaking via RCS limits the superconductivity from achieving an optimal state in $A_x(S)_y\text{TiNCl}$ compounds with $d < 20 \text{ \AA}$, causing $T_c < T_{c0}$.

Given this interaction model and structure, it is possible to explain all eight of the data points given in Fig. 3 of Ref. [6], including that of $\text{Li}_{0.13}\text{TiNCl}$, which does not follow the linear trend. In applying the model, one proceeds under the caveat that the results for T_c are obtained for compositions at or near optimal.

TABLE I. Structural and electronic parameters for $A_x(S)_y\text{TiNCl}$.

Compound	T_c (K)	d (Å)	d_2 (Å)	A (Å ²)	ζ (Å)	T_{c0} (K)	α (meV)	$T_c^{\text{calc.}}$ (K)
$\text{Na}_{0.16}\text{TiNCl}$	18.0	8.442	5.150	13.1564	1.6460	29.55	1.175	18.20
$\text{Na}_{0.16}(\text{THF})_y\text{TiNCl}$	10.2	13.105	5.183	12.9753	3.9610	12.36	0.230	10.35
$\text{Na}_{0.16}(\text{PC})_y\text{TiNCl}$	7.4/6.3	20.53	5.183	13.0331	7.6735	6.37	0	6.24
$\text{Na}_{0.16}(\text{BC})_y\text{TiNCl}$	6.9	20.7435	5.183	13.0331	7.7803	6.28	0	6.16
$\text{K}_{0.17}\text{TiNCl}$	17.0	8.778 84	5.182	13.3720	1.7984	27.65	1.086	16.84
$\text{Rb}_{0.24}\text{TiNCl}$	16.0	9.210 38	5.000	13.2830	2.1052	28.16	1.225	15.81
$\text{Li}_{0.13}(\text{THF})_y\text{TiNCl}$	9.5	13.0012	5.183	13.1277	3.9091	11.23	0.184	9.53
$\text{Li}_{0.13}\text{TiNCl}$	5.9	7.824 51	5.133	13.1277				

A. Optimal T_{c0}

High- T_c superconductivity in this model occurs in layered structures forming adjacent type-I and type-II charge reservoir layers containing the superconducting and mediating charges, respectively, repeating alternately along the transverse axis. The superconducting transition temperature depends on the spatially indirect Coulomb interaction across the transverse distance ζ between the two charge reservoirs, measured between the outer chlorines in the type-I $[\text{TiNCl}]_2$ layer and the locus of the cations A_x in the neighboring type-II intercalation layer, assuming co-intercalant $(S)_y$ is uncharged. The layered structure of $A_x(S)_y\text{TiNCl}$ is characterized by a thickness d_2 of the $[\text{TiNCl}]_2$ layers, the transverse spacing d between them, and an intercalant thickness $d - d_2$ [1]. Assuming that the mean cation A_x locus is at the intercalant-layer midplane, the interaction distance is $\zeta = (d - d_2)/2$. Since d_2 is approximately the same as for pristine $\alpha\text{-TiNCl}$ [1], the observed functional dependence of T_c on d is expected to correlate with an analogous dependence on ζ . However, one notes that the interlayer interaction length is the shorter distance ζ , rather than the spacing d . Structural and superconductivity data are presented in Table I, listing directly measured values of d_2 where available. The Coulomb energy e^2/ζ lies within 1.8–8.7 eV.

The doping-dependent optimization behavior, as generally exhibited by high- T_c compounds, suggests that optimization corresponds to equilibrium between the two reservoirs. The two-dimensional density of interaction charges is given in the model as $\sigma\eta/A$, where σ is the participating fractional charge in the type-I reservoir, determined per formula unit by doping as discussed below, η is the number of charge-carrying layers in the type-II reservoir and is given by $\eta = 1$ for $A_x(S)_y$, and A is the crystal basal-plane area per formula unit. Adopting this approach, it has been shown that the optimal transition temperature T_{c0} is given by the algebraic expression $k_B^{-1}\beta\zeta^{-1}(\sigma\eta/A)^{1/2}$, where $\beta = 0.1075(3) \text{ eV Å}^2$ is the universal constant determined previously by fitting experimental data [7]. The modeled T_{c0} is the upper limit on the experimentally observed transition temperature, given $T_c < T_{c0}$ for nonoptimal materials [10].

Particularly important to this model is the concept of the participating charge that is defined for optimal materials as the difference between the dopant charge stoichiometry and the minimum stoichiometric value required for superconductivity. An example is $x = 0.163$ taken relative to

$x_0 = 0$ in $\text{La}_{2-x}\text{Sr}_x\text{CuO}_{4-\delta}$. Doping is by direct cationic or anionic substitution in one or both reservoirs [11,12]. For $A_x(S)_y\text{TiNCl}$, doping occurs only in the intercalation layer via A_x such that σ is determined according to the simplified relation,

$$\sigma = \gamma|v(x - x_0)|, \quad (1)$$

where v is the valence and x is the optimal content of the cation dopant species in the type II $A_x(S)_y$ reservoir; x_0 is the threshold value of x for superconductivity; here, $v = 1$ for alkali-ion doping and $x_0 = 0$ is inferred from Refs. [1,6]. The factor γ derives from the allocation of the dopant by considering a given compound's structure. Following the procedure generally applied to high- T_c superconductors, the charge introduced by the dopant is shared equally between the two charge reservoirs. Additionally, the methodology requires the doped charge to be distributed pairwise between the charge-carrying layer types within each of the charge reservoirs. Assuming the co-intercalant contributes no doping charge, determination of γ for $A_x(S)_y\text{TiNCl}$ is comparable to that of $(\text{Ba}_{0.6}\text{K}_{0.4})\text{Fe}_2\text{As}_2$ [7] for which a structural analogy was previously noted [13]. Sharing the charge equally between the two reservoirs contributes a factor of 1/2 to γ . Sharing between the Cl layer and the double-TiN-layered structure and then to the two TiN layers contributes two factors of 1/2 to γ . Hence, $\gamma = (1/2)(1/2)(1/2) = 1/8$, yielding σ generally smaller than x .

B. Pair-breaking scattering

Although intercalation doping induces superconductivity in $A_x(S)_y\text{TiNCl}$, ΔT_c is broad and resistivity near T_c is high and semiconductorlike, e.g., data for $\text{Na}_{0.16}\text{TiNCl}$ show $T_c = 18.0 \text{ K}$, $\Delta T_c \approx 5 \text{ K}$ relative to the transition midpoint, and resistivity $\rho(T_c^+) \approx 0.27 \Omega \text{ cm}$ exhibiting an upturn as $\rho^{-1}T d\rho/dT \approx -0.3$ just above T_c [6]. Recognizing that the high measured resistivities have been attributed to the polycrystalline morphology of the samples under study [6,14], these are also signatures of high electron scattering rates τ^{-1} . A likely scattering mechanism is found by drawing analogy to modulation doping of semiconductor quantum wells [15] or RCS of carriers in a semiconducting inversion layer from fixed charges located outside the layer [9]. The form factor for the scattering process follows from the indirect Coulomb potential $v(q) \propto \exp(-qz)$, where q is the scattering wave vector and z is the transverse distance between the conducting

plane and the location of the Coulomb scattering center. Since the damping factor is obtained from an integration over potential fluctuations scaling with $|v(q)|^2$ [16], one expects in application of RCS to $A_x(S)_y\text{TiNCl}$ that $\hbar\tau^{-1}$ attenuates exponentially with the product of a characteristic value for q and z given by ζ or $d/2$.

Under conditions of strong scattering, particularly in the limit of small ζ where RCS would be strongest, it is possible that some fraction of the scattering contributing to $\hbar\tau^{-1}$ also induces pair-breaking scattering in the superconductor. Analogous pair-breaking effects in the cuprates originate from magnetic impurity scattering [17] and disorder associated with nonoptimization [10,18]. These pair-breaking effects, causing the observed depression of T_c below T_{c0} , are distinguished from weak scattering phenomena, which are less likely to affect T_c [19]. The following expression describes the pair-breaking affect on T_c [20], which has been applied to treat disorder in thin films [21] and the cuprates [10,18]:

$$\ln(T_{c0}/T_c) = \psi\left(\frac{1}{2} + \alpha/2\pi k_B T_c\right) - \psi\left(\frac{1}{2}\right). \quad (2)$$

Here, ψ is the digamma function, T_c is the experimentally measured transition temperature, T_{c0} is the optimal transition temperature calculated by assuming no pair breaking (Sec. II A), and α is the pair-breaking parameter. Thus, for a given compound with measured T_c and calculated T_{c0} , one obtains the associated α from Eq. (2).

Where the ionized intercalant induces RCS, pair-breaking is modeled by scaling α to the valence v and content x of species A_x and an exponential attenuation factor wherein the transverse distance is taken as ζ ,

$$\alpha = a_1 v x \exp(-k_1 \zeta). \quad (3)$$

Equation (3) is expressed in terms of empirical parameters, the coefficient a_1 and attenuation rate k_1 , which incorporate by approximation dependencies on scattering wave vector and screening as well as the finite thicknesses of the $[\text{TiNCl}]_2$ and $A_x(S)_y$ layers. In this model the pair-breaking rate, given by $2\hbar^{-1}\alpha$ [20], is expected to be small compared to the total scattering rate τ^{-1} associated with electrical transport.

In principle, screening dominates the strength of Coulomb scattering [9]. Because the bulk of the superconducting current flows in the $[\text{TiN}]_2$ substructures, one would expect T_c to vary significantly between the α and the β forms of $A_x(S)_y\text{MNX}$ and be modulated by the screening effects of the species M , X , and A , which increase with their atomic Z . The comparatively weaker cation screening available in the α -TiNCl compounds is expected to produce greater RCS-related suppression in T_c when compared to compounds based on β -ZrNCl or β -HfNCl, owing to the comparatively larger Z of Zr or Hf and larger d_2 of the β form [1]. This may account for results reported for Li_xZrNCl where mobilities and mean-free paths derived from $H_{c2}(T)$ data indicate minimal disorder scattering from the Li intercalant [15].

III. EXPERIMENTAL T_c

The starting point for understanding experimental results for T_c in $A_x(S)_y\text{TiNCl}$ is the optimal transition temperature

T_{c0} calculated for the unique optimal doping x ,

$$T_{c0} = k_B^{-1} \beta \zeta^{-1} [0.125v(x - x_0)/A]^{1/2}. \quad (4)$$

Using this model for T_{c0} in conjunction with the pair-breaking expression of Eq. (3), one may understand the variation in T_c with d for $A_x(S)_y\text{TiNCl}$ [6]. Since ζ depends functionally on d , correlations between T_c and d are thus possible, owing to the approximately constant d_2 (see Table I).

Zhang *et al.* [6] found that the correlation of T_c with $1/d$ breaks down for $\text{Li}_{0.13}\text{TiNCl}$, indicating that the length d is, perhaps, not the relevant length parameter involved. As d is not directly associated with a specific pair of interacting layers, this is not surprising. The key difference between d and ζ is that the former is always defined and nonzero, whereas the latter is unrealized in the absence of two physically separated and adjacent interacting layers. This subtle, but key, difference explains why $\text{Li}_{0.13}\text{TiNCl}$ does not behave in the same manner as the other seven compounds and provides strong support for the interlayer Coulomb interaction model described in Sec. II. Since the Li cations occupy sites between the Cl anions [6,22], a spatially separated intercalation layer is not formed; hence, $\text{Li}_{0.13}\text{TiNCl}$ does not possess the requisite two-layer interaction structure. The measured T_c is therefore hypothesized to reflect the BCS superconductivity of an intergrowth phase or inclusions related to TiN which has $T_c = 5.6$ K. This structural distinction also explains the absence of superconductivity in H_xZrNCl [23] where in this case the H impurities occupy the $6c$ site between the Zr-N and the Cl ions and dope the type-I reservoir; since the type-II reservoir is absent, high- T_c superconductivity does not occur. Nonsuperconducting Li-doped α -phase HfNBr appears to be a similar case in which localized spin paramagnetism is formed [24]. Additionally, Zhang *et al.* [6] compare their results with earlier studies of intercalated Bi-based cuprates [25] in which intercalation of charge-neutral molecules between the double BiO layers leaves T_c unchanged. Since ζ for the Bi-based cuprates is defined as the distance between adjacent SrO and CuO_2 layers [7], which does not change upon intercalation, this behavior is expected and confirms that ζ , not d , is the length which governs T_{c0} in high- T_c superconductors.

As evident from upturns in resistivity just above T_c , there exist large background scattering effects in the $A_x(S)_y\text{MNX}$ systems. High scattering rates can sometimes result in pair breaking via RCS interactions, degrading the superconducting state, and forcing T_c below T_{c0} . In particular, the α -TiNCl-based materials, exhibiting comparatively higher resistivities just above T_c [6], relative to those based on the β forms of ZrNCl [26,27] and HfNCl [5,14], are certainly good candidates. Following the logic set forth in Sec. II, the task becomes one of identifying and quantitatively extracting the pair-breaking component. To accomplish this, one first calculates T_{c0} assuming optimization; materials free of pair breaking and possessing the optimal cation doping necessarily exhibit $T_c = T_{c0}$ (within uncertainties). The suppression of T_c below T_{c0} evident in the remaining compounds can then be attributed to RCS-induced pair breaking or other pair-breaking phenomena.

Absent structural refinement data, the value of d_2 assumed from a related material or the host (see Fig. 4 and Table 4 of

Ref. [1]) is used in determining ζ . Values for ζ and T_{c0} from Eq. (4) are shown in Table I for the seven high- T_c compounds of Ref. [6]. As can be seen, only the two compounds with the largest ζ , $\text{Na}_{0.16}(\text{BC})_y\text{TiNCl}$ and $\text{Na}_{0.16}(\text{PC})_y\text{TiNCl}$, can be considered optimal, having $T_c \approx T_{c0}$ (Table I includes $T_c = 6.3$ K obtained by extrapolating $H_{c2}(T)$ for $\text{Na}_{0.16}(\text{PC})_y\text{TiNCl}$ in Fig. 2(b) of Ref. [6]), whereas the others show progressively larger deviations from optimal behavior with decreasing ζ . These deviations in $T_c < T_{c0}$, interpreted in terms of pair breaking, determine finite values of the pair-breaking parameter α as solutions of Eq. (2). The two compounds with $T_c \approx T_{c0}$ are taken to have $\alpha = 0$. The resulting values for α are listed in Table I. One finds that $A_x\text{TiNCl}$ without co-intercalation molecules exhibit the highest α values, 1.09–1.35 meV as expected for minimum ζ . The pair-breaking rate associated with 2α , which is less than 2.7 meV, is a very small component of the total scattering rate contained in $\hbar\tau^{-1}$. This can be ascertained, for example, by considering the damping factors $\hbar\tau^{-1} > 0.2$ eV indicated optically for Li_xZrNCl [28] and noting that transport measurements indicate higher resistivities for α -TiNCl-based compounds (e.g., $\rho(T_c^+) \approx 0.27$ Ω cm for $\text{Na}_{0.16}\text{TiNCl}$ [6]) when compared to β -ZrNCl-based compounds (e.g., $\rho(T_c^+) \approx 6.2$ m Ω cm for $\text{Li}_{0.08}\text{ZrNCl}$ [15]). Hence, these results are consistent with having $2\alpha \ll \hbar\tau^{-1}$.

In view of Eq. (3) based on the RCS model, the pair-breaking parameters for the seven $A_x(S)_y\text{TiNCl}$ compounds were scaled with doping in the form α/x ($v = 1$ for the alkali ions) and are plotted in Fig. 1 to show dependence on ζ . The curve is a fit to the function $a_1 \exp(-k_1 \zeta)$ with $a_1 = 23.9 \pm 1.0$ meV and $k_1 = 0.727 \pm 0.023$ \AA^{-1} , which displays remarkable representation of the data; the root-mean-square (rms) deviation between the α/x data and the corresponding function is 0.10 meV. In the limit where 2ζ approaches the van der Waals gap of pristine TiNCl (2.618 \AA) [1], the hypothetical maximum α of $(9.3 \pm 0.4$ meV) vx is also small compared to reasonable estimates of $\hbar\tau^{-1}$. The attenuation factor provides

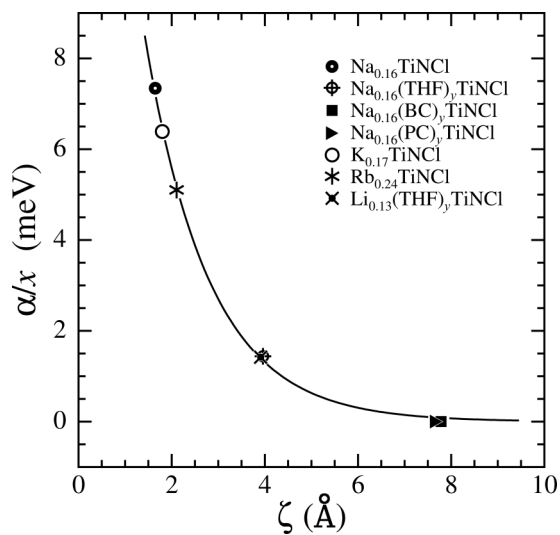


FIG. 1. Reduced pair-breaking parameter α/x plotted against interaction distance ζ for $A_x(S)_y\text{TiNCl}$. The curve is the fitted function of Eq. (3).

an estimate of the characteristic pair-breaking scattering wave vector as $\langle q \rangle = k_1/2 \sim 0.42 \pi A^{-1/2}$, suggesting large-angle scattering dominates ($\pi/A^{1/2} \approx 0.868$ \AA^{-1} from Table I). Modeling the distance z as $d/2$ in place of ζ in Eq. (3), yields $a_1 = 160 \pm 40$ meV, $k_1 = 0.736 \pm 0.042$ \AA^{-1} , and 0.18-meV rms deviation; the larger error obtained with $z = d/2$ correlates with the small variations in d_2 .

Evaluation of the linear trend between T_c and $1/d$ noted in Ref. [6] is readily obtained by fitting the function $T_c = s/d$ to the data for $A_x(S)_y\text{TiNCl}$ (excluding $\text{Li}_{0.13}\text{TiNCl}$), yielding $s = 145 \pm 4$ \AA K and rms deviation of 0.87 K in T_c . In comparison, the calculated transition temperature $T_c^{\text{calc.}}$, as determined by Eq. (2) with T_{c0} from Eq. (4) and α from Eq. (3), yields only 0.54-K rms deviation from measured T_c , indicating significant improvement for the model-based analysis over the heuristic scaling with $1/d$. The results for $T_c^{\text{calc.}}$ are given in Table I. Note that without RCS-related pair breaking, $T_c = T_{c0}$ and would approach 30 K for $A_x\text{TiNCl}$ without co-intercalant molecules.

IV. CONCLUSION

The very fine work of Zhang *et al.* [6] on α -form polymorphs $A_x(S)_y\text{TiNCl}$ is interpreted from the perspective of an interlayer Coulombic interaction model [7], identifying the superconducting [TiNCl] and mediating [$A_x(S)_y$] charge reservoirs, the relevant interaction distance ζ measured between cations A_x and Cl (different from the basal-plane separation d), and optimal transition temperature T_{c0} . Recognizing the presence of strong scattering from transport data, it is postulated that the transition temperatures could be suppressed due to pair breaking arising from the proximity of the superconducting layer to the dilute disordered charges of the intercalation layer. By adapting a pair-breaking model based on RCS, it is shown that the maximum attainable T_c ($\leq T_{c0}$) is determined by a unique pair-breaking parameter α , which falls off exponentially with increasing ζ . Not unexpectedly, the two compounds with the largest interaction distances, $\text{Na}_{0.16}(\text{PC})_y\text{TiNCl}$ and $\text{Na}_{0.16}(\text{BC})_y\text{TiNCl}$ ($\zeta = 7.6738$ and 7.7803 \AA , respectively), are found to be optimal with $T_c \approx T_{c0}$, whereas for the others (apart from $\text{Li}_{0.13}\text{TiNCl}$) RCS pair breaking is more dominant, owing to smaller ζ , yielding $T_c < T_{c0}$.

With the understanding that the important length governing T_c is ζ and not d , the anomalous behavior of Li_xTiNCl [6] and H_xZrNCl [23] is attributed to the location of the dopants in the [MNCI]₂ layers such that the physically separated mediating layer for high- T_c superconductivity is not formed and ζ is unrealized. This result suggests that the superconductivity observed in Li_xTiNCl is related to the BCS superconductivity of TiN ($T_c = 5.6$ K) [6,13,22].

ACKNOWLEDGMENTS

We are grateful for the support of the Physikon Research Corporation (Project No. PL-206) and the New Jersey Institute of Technology. We also thank Dr. S. Zhang and Professor R. F. Marzke for providing helpful and important information.

- [1] C. M. Schurz, L. Shlyk, T. Schleid, and R. Niewa, *Z. Kristallogr.* **226**, 395 (2011).
- [2] H. Kawaji, K. Hotehama, and S. Yamanaka, *Chem. Mater.* **9**, 2127 (1997).
- [3] T. Yokoya, T. Takeuchi, S. Tsuda, T. Kiss, T. Higuchi, S. Shin, K. Iizawa, S. Shamoto, T. Kajitani, and T. Takahashi, *Phys. Rev. B* **70**, 193103 (2004).
- [4] H. Tou, S. Oshiro, H. Kotegawa, Y. Taguchi, Y. Kishiume, Y. Kasahara, and Y. Iwasa, *Physica C Supercond.* **470**, S658 (2010).
- [5] S. Zhang, M. Tanaka, T. Onimaru, T. Takabatake, Y. Isikawa, and S. Yamanaka, *Supercond. Sci. Technol.* **26**, 045017 (2013).
- [6] S. Zhang, M. Tanaka, and S. Yamanaka, *Phys. Rev. B* **86**, 024516 (2012).
- [7] D. R. Harshman, A. T. Fiory, and J. D. Dow, *J. Phys.: Condens. Matter* **23**, 295701 (2011); **23**, 349501 (2011).
- [8] S. Yamanaka, *Annu. Rev. Mater. Sci.* **30**, 53 (2000).
- [9] T. Ando, A. B. Fowler, and F. Stern, *Rev. Mod. Phys.* **54**, 437 (1982).
- [10] D. R. Harshman and A. T. Fiory, *Phys. Rev. B* **86**, 144533 (2012).
- [11] D. R. Harshman and A. T. Fiory, *J. Phys.: Condens. Matter* **24**, 135701 (2012).
- [12] D. R. Harshman and A. T. Fiory (unpublished).
- [13] S. Yamanaka, *J. Mater. Chem.* **20**, 2922 (2010).
- [14] S. Zhang, M. Tanaka, H. Zhu, and S. Yamanaka, *Supercond. Sci. Technol.* **26**, 085015 (2013).
- [15] T. Takano, A. Kitora, Y. Taguchi, and Y. Iwasa, *Phys. Rev. B* **77**, 104518 (2008).
- [16] F. Gámiz, J. B. Roldán, J. E. Carceller, and P. Cartujo, *Appl. Phys. Lett.* **82**, 3251 (2003).
- [17] V. Z. Kresin, A. Bill, S. A. Wolf, and Y. N. Ovchinnikov, *Phys. Rev. B* **56**, 107 (1997).
- [18] D. R. Harshman, J. D. Dow, and A. T. Fiory, *Phys. Rev. B* **77**, 024523 (2008); **80**, 136502 (2009).
- [19] D. N. Basov, R. D. Averitt, D. van der Marel, M. Dressel, and K. Haule, *Rev. Mod. Phys.* **83**, 471 (2011).
- [20] M. Tinkham, *Introduction to Superconductivity*, 2nd ed. (McGraw Hill, New York, 1996).
- [21] A. F. Hebard and M. A. Paalanen, *Phys. Rev. B* **30**, 4063(R) (1984) and references cited therein.
- [22] S. Yamanaka, T. Yasunaga, K. Yamaguchi, and M. Tagawa, *J. Mater. Chem.* **19**, 2573 (2009).
- [23] S. Shamoto, K. Iizawa, T. Kato, M. Yamada, S. Yamanaka, K. Ohoyama, M. Ohashi, Y. Yamaguchi, and T. Kajitani, *J. Phys. Chem. Solids* **60**, 1511 (1999).
- [24] S. Yamanaka, H. Okumura, and L. Zhu, *J. Phys. Chem. Solids* **65**, 565 (2004).
- [25] P. J. Baker, T. Lancaster, S. J. Blundell, F. L. Pratt, M. L. Brooks, and S.-J. Kwon, *Phys. Rev. Lett.* **102**, 087002 (2009).
- [26] Y. Taguchi, A. Kitora, and Y. Iwasa, *Phys. Rev. Lett.* **97**, 107001 (2006).
- [27] M. Hiraishi, R. Kadono, M. Miyazaki, S. Takeshita, Y. Taguchi, Y. Kasahara, T. Takano, T. Kishiume, and Y. Iwasa, *Phys. Rev. B* **81**, 014525 (2010).
- [28] T. Takano, Y. Kasahara, T. Oguchi, I. Hase, Y. Taguchi, and Y. Iwasa, *J. Phys. Soc. Jpn.* **80**, 023702 (2011).